Journal of Clinical Imaging Science

Editor-in-Chief: Vikram S. Dogra, MD
Department of Imaging Sciences, University of Rochester Medical Center, Rochester, USA

OPEN ACCESS
HTML format

For entire Editorial Board visit : www.clinicalimagingscience.org/editorialboard.asp

www.clinicalimagingscience.org

ORIGINAL ARTICLE

Magnetic Resonance Imaging Analysis of Caudal Regression Syndrome and Concomitant Anomalies in Pediatric Patients

Deb K Boruah, Dhaval D Dhingani, Sashidhar Achar, Arjun Prakash[1], Antony Augustine, Shantiranjan Sanyal[2], Manoj Gogoi[3], Kangkana Mahanta

Departments of Radiodiagnosis and [3]Pediatric Surgery, Assam Medical College, Dibrugarh, Assam, [1]Department of Radiodiagnosis, NIMHANS, Bengaluru, Karnataka, [2]Department of Radiodiagnosis, RML and PGIMER, New Delhi, India

Address for correspondence:
Dr. Deb K Boruah,
RCC-4, M-Lane, Assam Medical College Campus, Dibrugarh, Assam - 786 002, India.
E-mail: drdeb_rad@yahoo.co.in

Received : 03-06-2016
Accepted : 18-08-2016
Published : 20-09-2016

ABSTRACT

Objective: The aim of this study was to evaluate the magnetic resonance imaging (MRI) findings of caudal regression syndrome (CRS) and concomitant anomalies in pediatric patients. **Materials and Methods:** A hospital-based cross-sectional retrospective study was conducted. The study group comprised 21 pediatric patients presenting to the Departments of Radiodiagnosis and Pediatric Surgery in a tertiary care hospital from May 2011 to April 2016. All patients were initially evaluated clinically followed by MRI. **Results:** In our study, 21 pediatric patients were diagnosed with sacral agenesis/dysgenesis related to CRS. According to the Pang's classification, 2 (9.5%) patients were Type I, 5 (23.8%) patients were Type III, 7 (33.3%) patients were Type IV, and 7 (33.3%) patients were of Type V CRS. Clinically, 17 (81%) patients presented with urinary incontinence, 6 (28.6%) with fecal incontinence, 9 patients (42.9%) had poor gluteal musculatures and shallow intergluteal cleft, 7 (33.3%) patients had associated subcutaneous mass over spine, and 6 (28.6%) patients presented with distal leg muscle atrophy. MRI showed wedge-shaped conus termination in 5 (23.8%) patients and bulbous conus termination in 3 (14.3%) patients above the L1 vertebral level falling into Group 1 CRS while 7 (33.3%) patients had tethered cord and 6 (28.6%) patients had stretched conus falling into Group 2 CRS. **Conclusion:** MRI is the ideal modality for detailed evaluation of the status of the vertebra, spinal cord, intra- and extra-dural lesions and helps in early diagnosis, detailed preoperative MRI evaluation and assessing concomitant anomalies and guiding further management with early institution of treatment to maximize recovery.

Key words: Lipomeningomyelocele, magnetic resonance imaging, sacral agenesis, tethered cord

Access this article online	
Quick Response Code:	Website: www.clinicalimagingscience.org
	DOI: 10.4103/2156-7514.190892

How to cite this article: Boruah DK, Dhingani DD, Achar S, Prakash A, Augustine A, Sanyal S, *et al*. Magnetic Resonance Imaging Analysis of Caudal Regression Syndrome and Concomitant Anomalies in Pediatric Patients. J Clin Imaging Sci 2016;6:36.
Available FREE in open access from: http://www.clinicalimagingscience.org/text.asp?2016/6/1/36/190892

INTRODUCTION

Caudal regression syndrome (CRS) is a rare congenital abnormality, in which a segment of the lumbar, lumbosacral, or coccygeal spinal agenesis or dysgenesis occurs in association with an abnormality in spinal cord and nerve roots.[1] In CRS, spectrum lumbosacral agenesis lies at the one end, and partial coccygeal agenesis lies at the other extreme of the spectrum. Various genitourinary, anorectal, Mullerian-duct, cardiovascular, orthopedic, and other spinal anomalies have been associated with CRS.

The progressive neurological deficits associated with CRS patients can be corrected with early diagnosis, detailed preoperative magnetic resonance imaging (MRI) evaluation of spine, spinal cord status and associated anomalies with early institution of treatment help in early recovery, especially in Pang Group 2 CRS patients.

It has been recognized that the degree of vertebral agenesis does not always correspond to the severity of coexisting genito-urinary, anorectal, and other neurogenic anomalies; hence, active search for other associated anomalies even in cases with mild degree of sacral agenesis is important by detailed MR evaluation as early correction of such anomalies might have profound effect on the clinical outcome of these patients.

The aim of this study was to evaluate the MRI findings in CRS and concomitant anomalies in pediatric patients.

MATERIALS AND METHODS

After approval from the Institutional Ethics Review Committee, a hospital-based cross-sectional retrospective study was conducted. The study group comprised 21 pediatric patients presenting to the Departments of Radiodiagnosis and Pediatric Surgery in a tertiary care hospital from May 2011 to April 2016.

Patient selection

We included both outpatients and inpatients up to the age of 16 years of both genders presenting with urinary, bowel, and spinal problems related to congenital or neuromuscular conditions. We have included only those children in whom imaging studies were performed. Children in whom imaging studies were not done were excluded from the study. Informed consent was obtained from parents/guardian before undergoing MRI scan.

Magnetic resonance imaging protocols

All patients were subjected to MRI scan using Siemens Avanto 1.5 Tesla B15 machine (Siemens Medical Systems, Erlangen, Germany). MRI of the spine was performed in sagittal, coronal, and axial planes using a combination of pulse sequences. MRI was performed with the patient in supine position with or without sedation under the guidance of anesthetist. Sagittal T2- and T1-weighted spin-echo images, sagittal short-tau inversion recovery (STIR), coronal STIR, and axial T2-, T1-weighted fast spin-echo images of the lumbosacral spine and pelvic regions were obtained routinely. Additional gradient-recalled echo (GRE) images were obtained in the sagittal plane in all patients for more detailed evaluation of vertebral defects or anomalies.

Sagittal spin-echo T1-weighted images (T1WIs) were acquired with 450–500/9–15 (repetition time/echo time). Sagittal T2-weighted images (T2WIs) were acquired with 4000–4600/110–120 (repetition time/echo time). All sagittal and coronal images were obtained with 3 mm slice thickness. Sagittal and coronal fat suppression sequences were employed on the long TR sequences. Sagittal GRE images were obtained with 650–750/24–32 (repetition time/echo time) with a flip angle of 24°–28°. Screening of brain was done in all patients.

Evaluation

Twenty-one CRS pediatric patients were examined to study the presence of congenital anomalies concomitant with CRS. The following conditions were given close attention: A family history of maternal diabetes mellitus, any medication used during pregnancy, a history of genetic illness, pediatric anorectal malformation, cleft mouth, diaphragm hernia, anomalies in the urinary, cardiovascular and respiratory systems, sirenomelia, spinal deformities such as lumbar, sacral, coccygeal partial or total agenesis/hypoplasia, or hip dysplasia.

On MRI, we evaluated type of CRS according to the Pang's classification, level of conus termination, shape of conus, causes of cord tethering or cord stretching, level of termination of thecal sac, height of syrinx formation in spinal cord according to vertebral height, vertebral segmentation defects, last present vertebra, anorectal malformation, or other associated anomalies. The presence of neurogenic bladder and hydroureteronephrosis was also evaluated.

Statistical analysis

Data were presented in terms of percentage and mean value. Calculations were done using Microsoft Excel.

RESULTS

In our study, 21 pediatric patients were diagnosed with sacral agenesis/dysgenesis related to CRS. Age of presentation varied from 3 days to 16 years with the

mean age of 5.36 year. Male: female sex ratio was 1:3.2. Mother of Pang Type I patients was diabetic. Clinically, 17 (81%) patients presented with urinary incontinence, 6 (28.6%) with fecal incontinence, 9 patients (42.9%) had poor gluteal musculatures and shallow intergluteal cleft, 7 (33.3%) patients had associated subcutaneous mass over spine, 5 (23.8%) patients had skin dimple over back, and 6 (28.6%) patients presented with distal leg muscle atrophy. According to the Pang's classification, 2 (9.5%) patients were defined as Type I, 5 (23.8%) patients were Type III, 7 (33.3%) patients were Type IV (5 were Type IVb and 2 were Type IVc), and 7 (33.3%) patients were defined as Type V CRS. According to conus termination, CRS patients were categorized into Groups I and II. MRI showed wedge-shaped conus termination in 5 (23.8%) patients [Figure 1] and bulbous conus termination in 3 (14.3%) patients [Figure 2] above the L1 vertebral level falling into Group 1 CRS while 7 (33.3%) patients had tethered cord and 6 (28.6%) patients had stretched conus falling into Group 2 CRS. The cause of tethered spinal cord in Group 2 CRS patients in our study was due to lipomeningomyelocele (Lipo-MMC) [Figure 3] in 4 (19%) patients, intraspinal lipoma in 2 (9.5%) patients, and 1 (4.8%) patient had terminal cystocele. Syrinx formation noted in 7 (33.3%) patients of Group 2 CRS, whereas 3 (14.3%) patients had syrinx <3 vertebral height and another 3 (14.3%) patients had >6 vertebral height.

Table 1 shows the MRI findings in CRS patients with concomitant spinal anomalies.

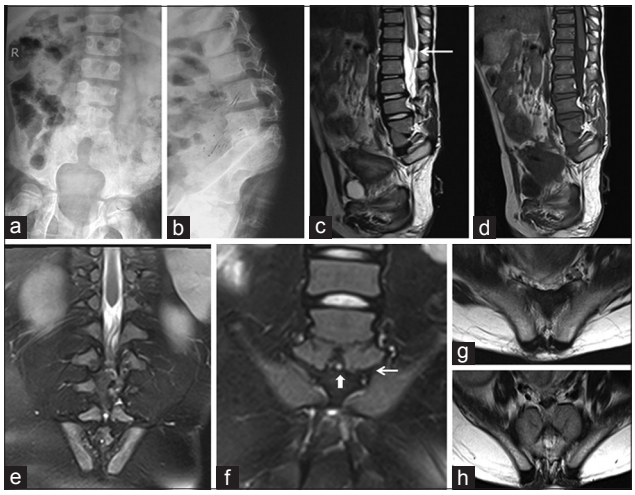

Figure 1: A 9-year-old male child with fecal incontinence, (a) and (b) X-ray anteroposterior and lateral views of lumbosacral spine shows the absence caudal spine with midline cleft in the lower lumbar vertebra. (c) Sagittal T2-weighted image, (d) T1-weighted image, and (e) coronal short-tau inversion recovery images show a complete absence of sacrococcygeal segments with a fusion between L4 and L5 vertebrae and wedge-shaped conus (← arrow) terminating at D12 vertebral level. (f) Coronal short-tau inversion recovery and (g and h) axial T2-weighted images show articulation in between iliac bones with L5 vertebra (← arrow) with a sagittal cleft in L5 vertebral body (↑ block arrow) representing Type I caudal regression syndrome.

Concomitant spinal or other system anomalies/conditions were demonstrated in our study as follows:

Genitourinary

Seventeen (81%) patients had a neurogenic bladder, 5 (23.8%) patients had bilateral hydroureteronephrosis, and 1 (4.8%) had a hypoplastic uterus (Type I Mullerian agenesis) [Figure 4].

Gastrointestinal

Nine patients (42.9%) had an imperforated anus, 8 (38.1%) had anorectal stenosis, 1 (4.8%) had anal stenosis, and 2 (9.5%) had a local anomaly [Figure 5], whereas one patient had omphalocele, cloacal exstrophy, imperforate anus, and spinal (OEIS) complex [Figure 6].

Associated other spinal dysraphism

Four (19%) patients with CRS had LipoMMC (1 had anterior LipoMMC), 4 (19%) had a high termination of thecal sac terminal above L5 vertebra, and 1 (4.8%) patient had a high termination of thecal sac above S1 vertebra. Six (28.6%) patients had tight filum terminale with fatty tissue which stretches the cord. One each of CRS patients had both intra- and extra-dural lipomas, intrasacral lipoma, diastematomyelia, terminal myelocystocele, both cervical intramedullary and intradural extramedullary neurenteric cysts [Figure 7], and intrasacral meningocele.

Vertebral anomaly

Fifteen (71.4%) CRS patients had vertebral segmentation defects, of which 13 (86.7%) patients had spina bifida, 4 (26.7%) had hemivertebra, 5 (33.3%) had butterfly vertebra, 2 (13.3%) had block vertebra, and 1 (6.7%) had reversed sacral curvature.

The present last vertebra in our study was S5 in 8 (38.1%) patients, S4 in 6 (28.6%) patients, S3 in 1 (4.8%) patient, S2 in 4 (19%) patients, and L5 in 2 (9.5%) patients.

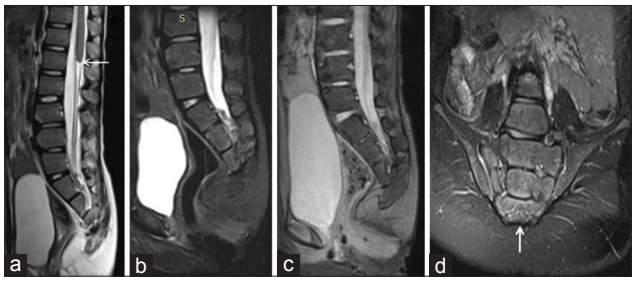

Figure 2: A 5-year-old female child with urinary incontinence, (a) sagittal T2, (b) short-tau inversion recovery, and (c) gradient recalled echo images show blind-ended spinal cord at L2 vertebral level (← arrow). (d) Coronal short-tau inversion recovery image shows the absence of coccyx and lowers two sacral segments bilaterally (↑ arrow) representing Type III caudal regression syndrome.

Table 1: The magnetic resonance imaging findings in caudal regression syndrome patients with concomitant spinal anomalies

Case	Age	Sex	CRS Type	Last vertebra	Level of conus	Conus shape	High thecal sac termination	T or intraspinal lesion	Other anomaly
1	9 years	Male	I	L5	D12	W	L3	No	Triangular pelvis
2	3 days	Male	V	S5	Sacrococcygeal junction	T	No	Terminal myelocystocele	Cloacal anomaly with reversed sacral curvature
3	2 years	Female	IVc	S4	Lower border of L1	W	No	No	Pubic diastasis
4	3 years	Female	I	L5	D12	B	L4	No	No
5	5 years	Male	V	S5	D12	W	L5	ID and IM NEC in cervical region	No
6	10 months	Female	IVc	S4	L2	W	No	ID and extradural lipoma	Anal atresia
7	14 years	Female	III	S4	L2	S	No	No	Mullerian agenesis I
8	7 months	Female	III	S4	Lower border of L2	W	No	Intrasacral lipoma	Cloacal anomaly
9	3 years	Female	III	S2	Upper border of L1	B	L5	No	Intergluteal cyst
10	4 years	Female	IVb	S2	S2	T	No	LipoMMC	Left buttock fatty mass
11	5 years	Female	III	S3	L1	B	No	No	No
12	16 years	Male	IVb	S2	Lower border of S2	T	No	LipoMMC with ID lipoma	Left buttock fatty mass
13	11 years	Female	IVb	S2	S2	T	No	LipoMMC	No
14	6 years	Female	V	S5	S2	S	No	Diastematomyelia	Skin dimple with tuft of hair
15	16 days	Female	V	S5	S2	S	No	No	Anorectal atresia with rectovestibular fistula
16	16 years	Female	III	S4	S2	S	No	Intrasacral lipoma	Left buttock fatty mass
17	2 years 6 months	Female	IVb	S4	S2	T	S1	No	No
18	9 years	Male	V	S5	L2	S	No	No	No
19	3 months	Female	V	S5	S5	T	No	LipoMMC	Right buttock fatty mass
20	28 days	Female	V	S5	L2	S	No	No	Pubic diastasis
21	3 years	Female	IVb	S5	S3	T	No	LipoMMC	Right buttock fatty mass

W: Wedge, B: Blunted, S: Stretched, T: Tethered, LipoMMC: Lipomeningomyelocele, NEC: Neurenteric cyst, ID: Intradural, IM: Intramedullary, CRS: Caudal regression syndrome

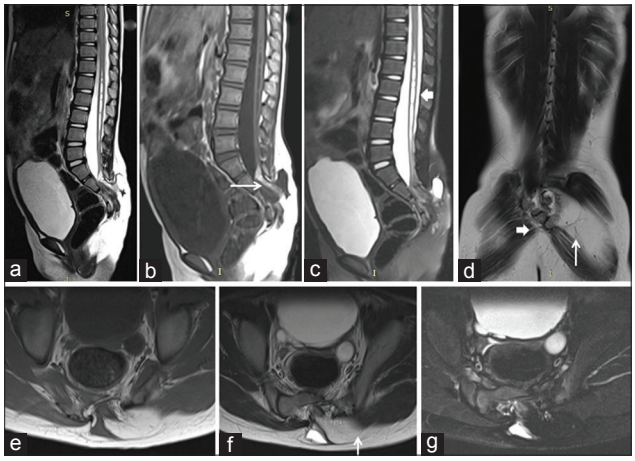

Figure 3: A 4-year-old female child with left buttock swelling, (a) sagittal T2-weighted image, (b) T1-weighted image, and (c) short-tau inversion recovery images show T1 and T2 hyperintense fatty tissue mass in sacral spinal canal (→ arrow) causing tethering of spinal cord with T1 hypo- and T2 hyper-intense syrinx formation (← block arrow). (d) Coronal T2-weighted image, (e) axial T1-weighted image, (f) axial T2-weighted image, (g) axial fat-suppressed T2-weighted images show the extension of fatty tissue via sacral defect into left buttock (↑ arrow). The absence of coccyx and left-sided lower sacral segments is noted beyond S2 vertebra (→ block arrow) representing Type IVb caudal regression syndrome.

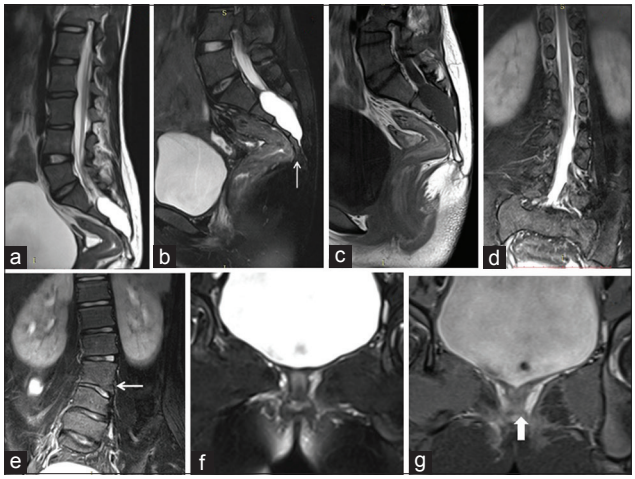

Figure 4: A 14-year-old female with primary amenorrhea. (a) Sagittal T2-weighted image, (b) short-tau inversion recovery, (c) T1-weighted images show a lobulated T1 hypo- and T2 hyper-intense intrasacral meningocele in the lower sacral spinal canal with the absence of coccyx and bilateral S5 segments of the sacrum (↑ arrow) representing Type III caudal regression syndrome. (d and e) Coronal short-tau inversion recovery images show L3 hemivertebra (← arrow) and low-lying spinal cord ended at L2 vertebral level. (f) Coronal fat-suppressed T2-weighted image and (g) coronal short-tau inversion recovery images show hypoplastic uterus (↑ block arrow) of Type I Mullerian anomaly.

Musculoskeletal

Two CRS patients had pubic diastases, and one patient had bilateral congenital talipes equinovarus.

Miscellaneous

One CRS Type III patient had associated T1WI hypo- and T2WI hyper-intense intergluteal cleft cyst [Figure 8]. Brain

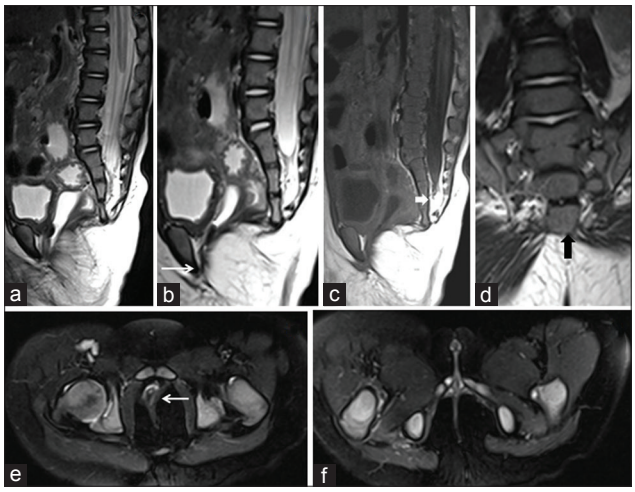

Figure 5: A 7-month-old female infant with fecaluria, (a and b) sagittal T2-weighted image, (c) T1-weighted images show common opening of urethral, vaginal, and atretic anus representing a local anomaly (→ arrow) with intradural lipoma (→ block arrow) in sacral canal causing low-lying tethered cord, where conus ended at L2 vertebral level. (d) Coronal T2-weighted images show complete S5 and coccygeal agenesis with truncation of the thecal sac at S1 vertebral level representing Type III caudal regression syndrome. (e and f) Axial fat-suppressed T2-weighted images show thinned out bilateral perineal muscles with the atrophied perineal body (← arrow).

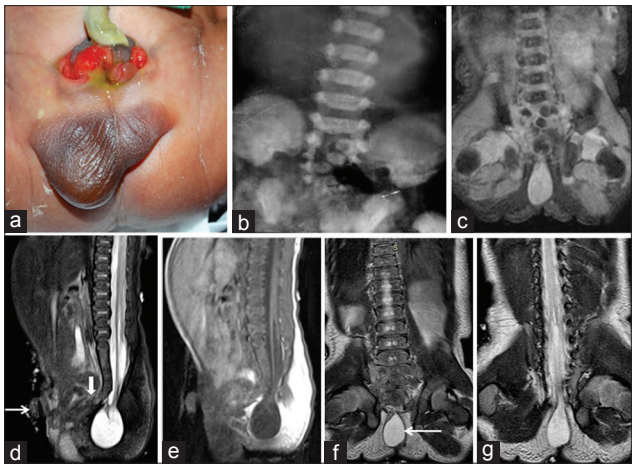

Figure 6: A 3-day-old male infant, (a) photograph of the patient shows omphalocele and bladder exstrophy. (b) X-ray anteroposterior view of the lumbosacral spine and (c) coronal gradient-recalled echo images show segmentation defects in the sacrum. (d) Sagittal short-tau inversion recovery, (e) T1-weighted image, (f and g) coronal T2-weighted images show T1 hypo- and T2 hyper-intense terminal myelocystocele (← arrow) with tethered cord and anterior abdominal wall defects and herniation of bowel loops (→ arrow). Reversed sacral curvature is noted with agenesis of coccygeal segments (↓ block arrow) representing omphalocele, cloacal exstrophy, imperforate anus, and spinal complex with Type V caudal regression syndrome.

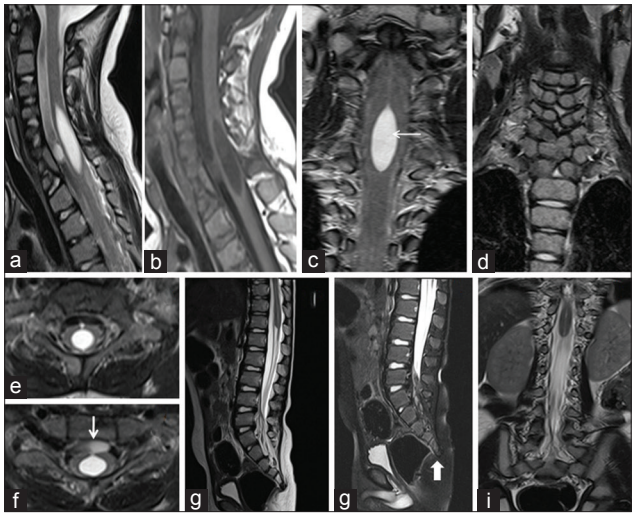

Figure 7: A 5-year-old male child with quadriparesis, (a) sagittal T2-weighted image, (b) T1-weighted image, and (c) coronal T2-weighted images show a T1 hypo- and T2 hyper-intense cyst within cervicodorsal cord (← arrow). (d) Coronal T2-weighted images show segmentation defects in C3 to D1 vertebrae. (e and f) Axial T2-weighted images show smaller cyst in anterior epidural space at C7 vertebral level with a thin communication between the extra- and intra-medullary cysts (↓ arrow). (g) Sagittal T2-weighted images, (h) short-tau inversion recovery, and (i) coronal T2-weighted images show a complete absence of coccyx (↑ block arrow) with conus terminating at the D12 vertebral level, representing Type V caudal regression syndrome.

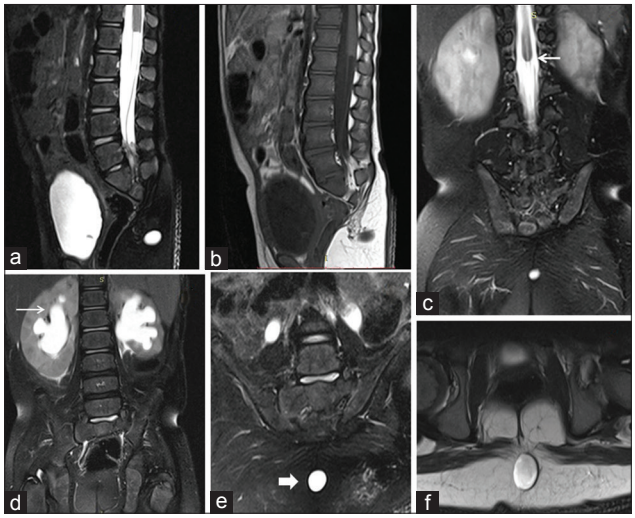

Figure 8: A 3-year-old female child with a shallow natal cleft, (a) sagittal short-tau inversion recovery, (b) T1-weighted image, and (c) coronal short-tau inversion recovery images show sacrococcygeal agenesis with rudimentary S2 vertebra with blind-ended conus (← arrow) representing Type III caudal regression syndrome. (d) Coronal short-tau inversion recovery image shows bilateral hydroureteronephrosis (→ arrow). (e) Coronal short-tau inversion recovery and (f) axial T2-weighted images T2 hyperintense midline cystic lesion in intergluteal cleft (→ block arrow).

screening showed Type II Chiari malformation in a patient of Type III CRS.

DISCUSSION

CRS is an uncommon malformation of the caudal spine and spinal cord malformation. CRS comprises developmental anomalies of the caudal vertebrae, neural tube, urogenital and digestive organs, and hind limbs, the precursors of all of which are derived from the caudal eminence.[2] Its incidence is estimated approximately 0.1–0.25:10,000 of normal pregnancies.[3] The incidence is higher about 1:350 infants of diabetic mothers and which representing an increase of risk about 200 times.[3-5] The CRS had a male: female ratio of 2.7:1.[6]

The term CRS was first used in 1961 by Duhamel[7] to describe a syndrome incorporating vertebral agenesis of the variable level with urinary and digestive malformations. Pregestational diabetes is undoubtedly a teratogen, and there is good evidence that gestational diabetes can be involved in the development of the most severe form of CRS.[8] The other possible risk factors include genetic susceptibility and vascular hypoperfusion.[9]

The degree of spinal cord aplasia correlates with the severity of the spinal malformation, with a greater degree of vertebral aplasia in Group 1 than in Group 2.[10]

Clinically, most patients with sacral agenesis exhibit poorly developed "rumps" with short, shallow intergluteal clefts and poor gluteal musculature. They show narrow hips, distal leg atrophy, and talipes deformities. Approximately 20% have subcutaneous lesions such as skin-covered lipomeningoceles (6%), terminal myelocystoceles (9%), or limited dorsal myeloschisis (3%).[11] In our study, we encountered 33.3% of patients with CRS had subcutaneous mass.

Various genitourinary, gastrointestinal, musculoskeletal, and cardiothoracic anomalies are associated with caudal spinal agenesis or dysgenesis.

Motor deficits are present and correspond to the level of vertebral agenesis.[12] The sensation is better preserved in CRS patients than somatic motor function.[13,14] The discrepancy between neurological symptoms and the extent of the spinal defect may be due to the persistence of nerve fibers beneath the vertebrae or enhanced capabilities of sensitive ganglions.[15] Urinary and bladder dysfunctions are constant with CRS.[11]

Agenesis of the sacrococcygeal spine may be a part of syndromic complexes such as OEIS,[16] VACTERL (vertebral abnormality, anal imperforation, cardiac anomalies, tracheoesophageal fistula, renal abnormalities, and limb deformities),[16,17] and the Currarino triad (partial sacral agenesis, anorectal malformation, and presacral mass: teratoma and/or meningocele).[9,18,19]

Antenatal ultrasound (USG) diagnosis of CRS is possible at the end of the first trimester.[20] Inappropriate crown-rump length may be the first sign of CRS in the first trimester. At a later stage, USG findings include abrupt interruption of the spine at dorsal, lumbar, or sacral level with the femurs fixed in a characteristic "V" pattern due to external rotation of the hip joints ("Buddha's attitude").[20,21]

The Pang's classification of lumbosacral agenesis with five types: where Types I and II represent total sacral agenesis with and without associated lumbar vertebral agenesis; Type III represents subtotal sacral agenesis with at least S1 present; Type IV has a hemisacrum; and Type V includes coccygeal agenesis.[11]

In Group 1 (41%), the conus ends cephalic to the lower border of L1. In Group 1 with high conus, the sacral deficit is typically large, and the sacrum usually ends at or above S1. These patients have a stable neurological defect due to their "fixed" spinal cord dysplasia. In Group 2 (59%), the conus ends lower, below L1, and is elongated, stretched caudally, and tethered. Progressive neurological deterioration is frequent in these patients due to the low-tethered cord.[22] In our study, 8 patients (38.1%) had conus termination above the L1 vertebral level falling into Group 1 while 13 patients (61.9%) had tethered or stretched low-lying conus falling into Group 2.

The dural sac in CRS patient shows nonstenotic tapering and shortening in around 47% cases. The tapering is greater, and the sac ends higher with higher levels of spinal agenesis.[11] In our study, 5 (23.8%) patients had a high termination of the thecal sac.

Even plain radiography and computed tomography of spine more readily determine osseous anomalies, MR effectively depicts the levels of vertebral agenesis, and it also allows exact identification of dysgraphic-dysplastic anomalies in all patients.[10]

Management is primarily directed toward correction of genitourinary and anorectal anomalies with the goals being to preserve renal function, achieve continence, and prevent infection. Surgical untethering, release, or neuroplasty are procedures that may be necessary to improve neurological function in CRS patients.

Limitations

We could not perform MRI in many cases of clinically suspected spinal dysraphism or caudal spinal anomalies due to cost constraints and those patients who were not suitable for sedation by an anesthesiologist.

CONCLUSION

MRI is the ideal modality for detailed evaluation of the status of the vertebra, spinal cord, intra- and extra-dural lesions, and associated concomitant anomalies of pediatric CRS patients and helps in guiding further management of CRS.

In MRI, a thorough search for caudal spinal, anorectal, and genitourinary anomalies should be pursued even with milder vertebral agenesis if patient presents with progressive neurologic deficits.

In our study of 21 pediatric patients diagnosed as CRS, MRI allowed us to see the various concomitant conditions which often occur with CRS.

A better understanding of such coexisting pathologies with the help of MRI will allow us to not only prevent a progressive neurological deficit in relevant cases at an early stage but also focus attention toward the correction of other associated anomalies. Apart from complex intradural and neurogenic anomalies, detection of other genitourinary and anorectal anomalies helps the clinicians to have an overall assessment of the case and its prognosis earlier, decide management, and counsel the family members accordingly.

Financial support and sponsorship

Nil.

Conflicts of interest

There are no conflicts of interest.

REFERENCES

1. Tortori-Donati P, Fondelli MP, Rossi A, Raybaud CA, Cama A, Capra V. Segmental spinal dysgenesis: Neuroradiologic findings with clinical and embryologic correlation. AJNR Am J Neuroradiol 1999;20:445-56.
2. Padmanabhan R. Retinoic acid-induced caudal regression syndrome in the mouse fetus. Reprod Toxicol 1998;12:139-51.
3. Sen KK, Patel M. Caudal regression syndrome. Med J Armed Forces India 2007;63:178-9.
4. Kucera J. Rate and type of congenital anomalies among offspring of diabetic women. J Reprod Med 1971;7:73-82.
5. Jaffe R, Zeituni M, Fejgin M. Caudal regression syndrome. Fetus Spinal Anom 1991;7561:1-3.
6. Stevenson RE, Jones KL, Phelan MC, Jones MC, Barr M Jr., Clericuzio C, et al. Vascular steal: The pathogenetic mechanism producing sirenomelia and associated defects of the viscera and soft tissues. Pediatrics 1986;78:451-7.
7. Duhamel D. From the mermaid to anal imperforation: The syndrome of caudal regression. Arch Dis Child 1961;36:152-5.
8. Versiani BR, Gilbert-Barness E, Giuliani LR, Peres LC, Pina-Neto JM. Caudal dysplasia sequence: Severe phenotype presenting in offspring of patients with gestational and pregestational diabetes. Clin Dysmorphol 2004;13:1-5.
9. Gabbe SG, Niebyl JR, Simpson JL. Obstetrics: Normal and Problem Pregnancies. 4th ed. New York: Churchill Livingstone; 2002.
10. Nievelstein RA, Valk J, Smit LM, Vermeij-Keers C. MR of the caudal regression syndrome: Embryologic implications. AJNR Am J Neuroradiol 1994;15:1021-9.
11. Pang D. Sacral agenesis and caudal spinal cord malformations. Neurosurgery 1993;32:755-78.
12. Dias MS, McLone DG, Partington M. Normal and abnormal embryology of the spinal cord and spine. In: Winn HR, editor. Youmans Neurological Surgery. 5th ed., Vol. 4. Philadelphia: WB Saunders; 2003. p. 4239-88.
13. Hudson LP, Ramsay DA. Malformation of the lumbosacral spinal cord in a case of sacral agenesis. Pediatr Pathol 1993;13:421-9.
14. Sarnat HB, Case ME, Graviss R. Sacral agenesis. Neurologic and neuropathologic features. Neurology 1976;26:1124-9.
15. Subtil D, Cosson M, Houfflin V, Vaast P, Valat A, Puech F. Early detection of caudal regression syndrome: Specific interest and findings in three cases. Eur J Obstet Gynecol Reprod Biol 1998;80:109-12.
16. Carey JC, Greenbaum B, Hall BD. The OEIS complex (omphalocele, exstrophy, imperforate anus, spinal defects). Birth Defects Orig Artic Ser 1978;14:253-63.
17. Smith NM, Chambers HM, Furness ME, Haan EA. The OEIS complex (omphalocele-exstrophy-imperforate anus-spinal defects): Recurrence in sibs. J Med Genet 1992;29:730-2.
18. Currarino G, Coln D, Votteler T. Triad of anorectal, sacral, and presacral anomalies. AJR Am J Roentgenol 1981;137:395-8.
19. Gudinchet F, Maeder P, Laurent T, Meyrat B, Schnyder P. Magnetic resonance detection of myelodysplasia in children with Currarino triad. Pediatr Radiol 1997;27:903-7.
20. Baxi L, Warren W, Collins MH, Timor-Tritsch IE. Early detection of caudal regression syndrome with transvaginal scanning. Obstet Gynecol 1990;75 (3 Pt 2):486-9.
21. Twickler D, Budorick N, Pretorius D, Grafe M, Currarino G. Caudal regression versus sirenomelia: Sonographic clues. J Ultrasound Med 1993;12:323-30.
22. Tortori-Donati P, Rossi A, Biancheri R, Cama A. Magnetic resonance imaging of spinal dysraphism. Top Magn Reson Imaging 2001;12:375-409.